A Post-Design of Topology Optimization for Mechanical Compliant Amplifier in MEMS

C. F. Lin and C. J. Shih*

Department of Mechanical and Electro-Mechanical Engineering, Tamkang University, Tamsui, Taiwan 251, R.O.C.

Abstract

The topology synthesis approach can generate a creative initial optimized configuration and can generate approximately well locations of hinges. It is particularly useful to form a monolithic compliant mechanism in MEMS application. However, the formation of hinges-like portion is typically encountered as a major unsolved problem. Such hinges unavoidably exist in the topological layout but cannot practically manufacture. This paper proposes an approach using the analytic single-axis flexure hinge integrated with the formal optimization as a post-design process to obtain optimum flexure hinges and its location for promoting the overall performance. A compliant micro gripper/magnifying mechanism is adopted as an example to illustrate the presenting approach; and a multi-objective optimization problem consisting of several constraints are constructed to determine nine unknowns. The numerical experiment shows the proposed post-optimum design is effective and can be utilized to other similar design situation.

Key Words: Flexure Hinge, Compliant Mechanism, Engineering Optimization, MEMS, Mechanical Design

1. Introduction

Micro electro-mechanical systems (MEMS) are built in sub-millimeter scale and integrated with electronic circuits. Compliant mechanisms are single-piece flexible structures and well suited for MEMS because of the small length scale and problems with assembly, friction and wear that prohibit use of conventional rigid-body mechanisms [1]. Compliant mechanisms are a relatively new class of mechanisms that utilize compliance of their constituent elements to transmit motion and/or force. They can be designed for any desired input-output force-displacement characteristics, including specified volume/weight, stiffness, and natural frequency constraints. As flexure is permitted in these mechanisms, they can be readily integrated with unconventional actuation schemes, including thermal, electrostatic, piezoelectric, and shape-memory-alloy actuators [2].

Most piezoelectric ceramic materials can only produce a maximum strain level of 0.1%. Hence, various approaches have been developed to increase the actuation stroke in these materials for practical applications. One approach employs mechanical amplifiers (amplifying mechanism) to magnify actuation produced by standard piezoelectric ceramics. Figure 1 indicates an integration of a piezoelectric actuator with an amplification transmission device that was designed to provide 20:1 amplification using energy method [2] and is effective to modify the force-displacement characteristics. As the amplify-

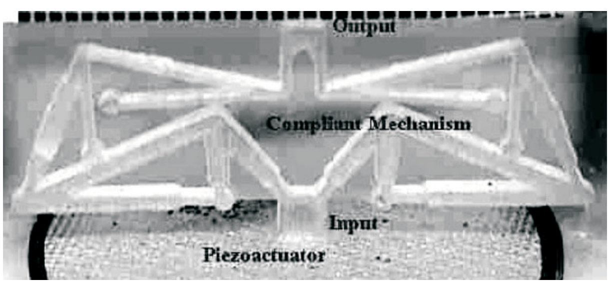

Figure 1. Piezoceramic actuator integrated with 20:1 stroke amplification mechanism [2].

*Corresponding author. E-mail:cjs@mail.tku.edu.tw

ing mechanism is designed to be monolithic, it can be considered a kind of compliant mechanism. Hence, topology optimization techniques [1,3–5] developed for compliant mechanisms can be directly applied to the design of amplifying mechanisms.

Topology optimization has been successfully used to solve various structural problems. A typical development of using topology optimization is to systematically design mechanical amplifiers, such as the force amplifier [6], elliptic elastic amplifier and dot-matrix printers [7]. The results of the topology optimization then are converted to beam element models that are used for a further modification. For the example of the elliptic elastic amplifier, an optimum topology for the maximum magnification factor driven at excitation frequencies 30 Hz is shown on Figure 2(a). This topological layout was modified by experiences that in place of single-node connection or very thin flexures were made of continuum components and with reasonable thickness, as shown in Figure 2(b) [6]. Figure 2(b) shows the finite element analysis by ANSYS in which the interpreted mechanism as a broken line and the deformed mechanism as a full line. In this case, the topology optimization can provide an initial configuration of the mechanical amplifier. The final design for manufacturing requires further refined modification by some skilled engineering drafting. Thus, the final result in Figure 2(b) has no effort to the critical section design of flexure hinge portion, in the meanwhile; it is not an optimum design.

There are two major problems arises in numerical topology synthesis. The first problem is checkerboard formation [8] should be carefully dealt with in order to obtain satisfactory results. Another numerical problem encountered in the topology optimization of compliant mechanisms is the formation of single-node that should not be the part of final designs especially in the area of MEMS. Figure 3 shows the topological design of a force inverter [9] without checkerboard control. One can see the mark with a circle indicates the portion of hinge-like single-node. Such the point actually represents the hinge to possess a localized compliant behavior that is unrealizable in a real mechanical system. Several works for preventing hinge formation of single-node have been proposed in recent years [1,10–12]. An alternative procedure by Yoon et al [9] in which a multi-scale wavelet-based topology optimization formulation to obtain hinge-free result was presented. This post-processing can change the portion of single-node (indicated in Figure 4(a)) to a design (indicated in Figure 4(b)) for a compliant hinge. The design in Figure 4(b) indeed takes away the singular hinge portion, however, it still not conform to the configuration of the real mechanical flexure hinge.

A practical mechanically compliant flexure joint is included in a flexure-based gripper, as illustrated in Figure 5 [13]. Under a small deflection, the flexure joint can be

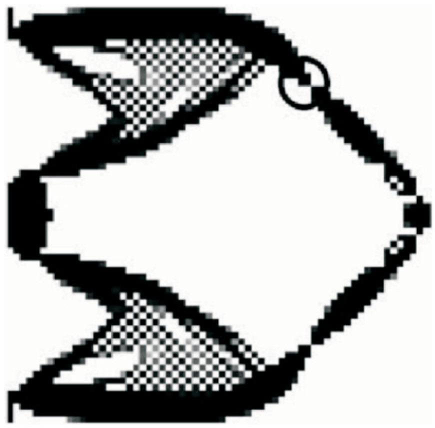

Figure 3. Force inverter topological design [9].

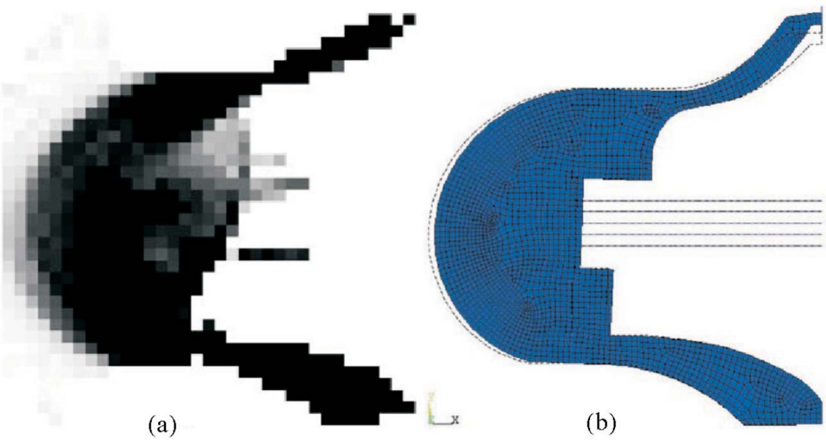

(a) (b)

Figure 2. Optimum topology of the elliptic elastic amplifier [7].

Figure 4. (a) A single-node hinge (b) Compliant hinge by post-processing [9].

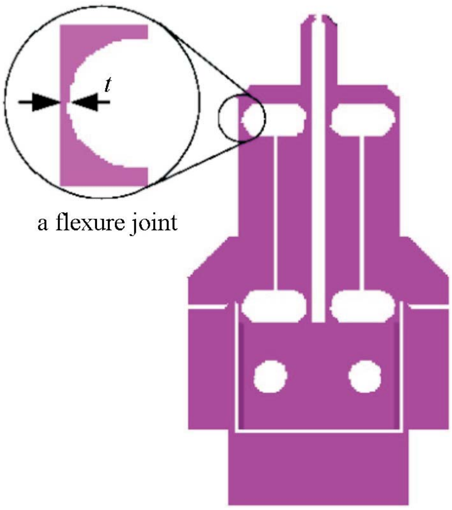

Figure 5. Flexure based gripper mechanism [13].

modeled as a rigid hinge joint attached by a linear torsional spring for the analysis and design, as shown in Figure 6 [13]. This idea inspires us to re-examine the formulation of a mechanical flexure hinge directly applies to the post-topology optimization of a compliant mechanism design. This paper presents such the post-processing technique of optimizing the mechanical flexure hinge and its surrounding area to promote the overall performance of a compliant structure. A compliant micro-gripper acting as

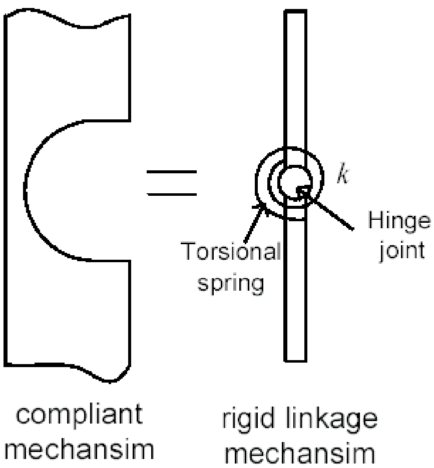

Figure 6. Flexure joint modeling [13].

a mechanical amplifier is employed as the example to illustrate the proposed post-optimization approach.

2. Mechanics of Flexure Hinge

The geometrical shape surrounding the flexure hinge is critical for the output performance of a single-piece compliant mechanism, as recognized by researchers. Figure 7 shows dimensions that define the hinge, various forces and moments for which the angular and linear compliances are calculated. A single-axis flexure hinge must be flexible about the input axis or sensitive axis. Usually, the hinge must be as stiff as possible about the cross axis and along the longitudinal axis.

For an input moment M_z causes the flexure to deflect through angle α_z. The simplified compliance equation can be derived as:

$$\frac{\alpha_z}{M_z} \approx \frac{9\pi R^{0.5}}{2Ebt^{2.5}} \tag{1}$$

For practically any hinge, the error will be less than 1 percent as compared with original complicated formulation [14]. The equivalent torsional spring rate can be written as:

$$K_\theta = \frac{M_z}{\alpha_z} \approx \frac{2Ebt^{2.5}}{9\pi R^{0.5}} \tag{2}$$

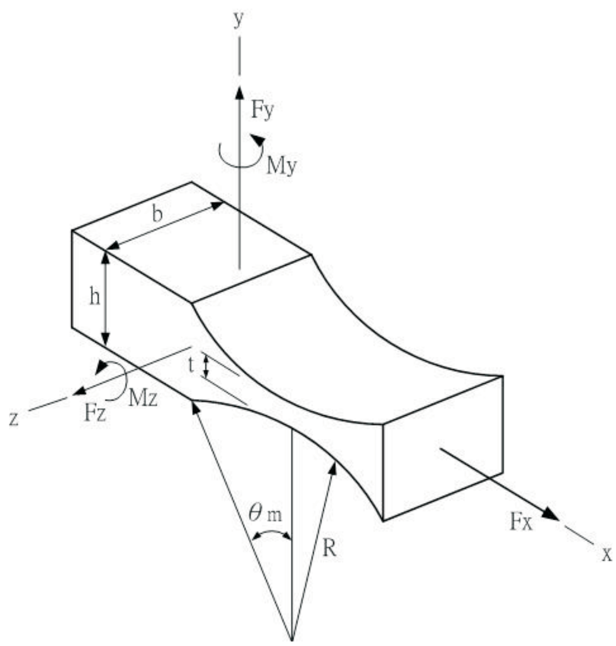

Figure 7. Hinge dimensions and various forces and moments.

Linear deflection Δy may be caused by moment M_z. Thus, the simple form of compliance for the case of applied moment is:

$$\frac{\Delta y}{M_z} \approx \frac{9\pi R^{1.5}}{2Ebt^{2.5}} \tag{3}$$

The equivalent linear spring rate along y-direction can be written as:

$$K_y = \frac{M_z}{\Delta y} \approx \frac{2Ebt^{2.5}}{9\pi R^{1.5}} \tag{4}$$

The hinge height h is not important factor in angular compliance and linear compliance. This single-axis flexure has been used more popular than two-axis flexure.

3. Topology Synthesis of Compliant Structure

A general compliant mechanism design problem is sketched in Figure 8. A spring at the output port simulates the resistance from the work-piece. The goal of the optimization problem is to maximize the work performed on the spring. A topology optimization solving the problem of distributing a limited amount of material in the design domain such that the output displacement is maximized can be written as:

$$\max f(X) = U_{out}(\rho) \tag{5}$$

$$\text{s.t.} \sum_{i=1}^{N} \rho_i v_i \le V \tag{6}$$

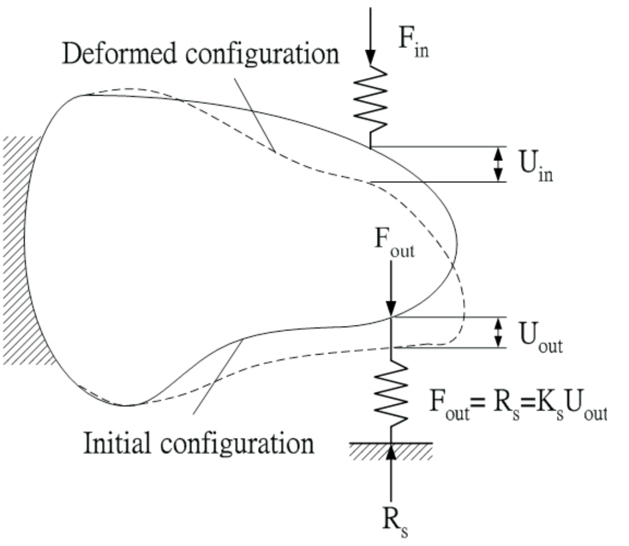

Figure 8. Domain for a compliant mechanism design.

$$0.001 \le \rho_i \le 1 \tag{7}$$

where the V is the upper limit of the required material volume. In the optimization process, the relation of {F} = [K]{U} must be satisfied. The relative density in each element, indicated as ρ_i, is a design variable. The N-vector containing the design variables is denoted as ρ.

In this paper, the design of a compliant micro-gripper/magnifying mechanism is the example for the demonstration. The design domain is sketched in Figure 9. The grey area denotes the quadratic design domain that is supported at the left edge. The size of the design domain is 3.2 × 1.82 mm^2 and the thickness is 0.2 mm. The gripper is built in PU material that has Young's modulus 7.775 × 10^7 Pa and poison ratio 0.4669. An input force F_{in} = 0.2 g is applied at the center of 1.06 mm from the left edge and the output spring (0.031 N/mm) is mounted at the output of the right edge. The material property and the overall size is the same as the thesis of Tsao [15]. The input spring is 46.65 N/mm and the material volume is restricted to be 30 per cent of the design domain. Due to symmetry, only the half of the design domain is discretized using 3210 4-node finite elements. The optimized topology synthesis can be obtained and shown in Figure 10.

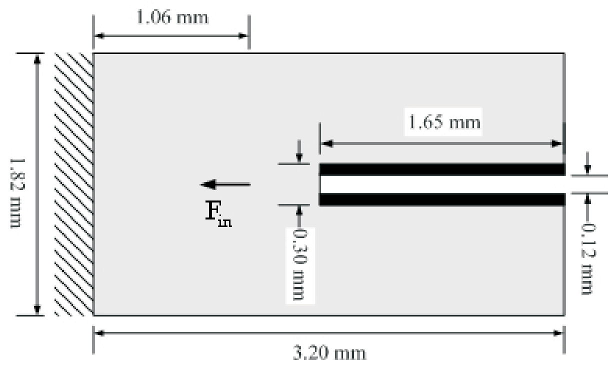

Figure 9. Design domain for the micro gripper amplifying mechanism.

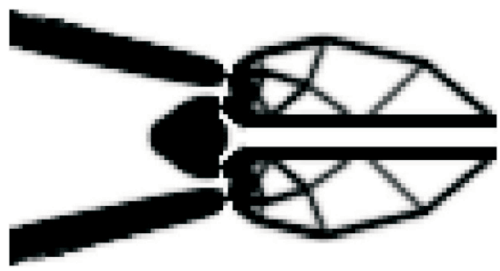

Figure 10. Topology synthesized micro gripper mechanism.

4. Post-Design Modeling of Optimization for Compliant Structure

Two elliptic circles are marked on the Figure 11 that shows hinge-like portions, as enlarged picture shown, required to be modified in practical application. How can one modify the hinge-like portion to be a mechanical compliant flexure-hinge for manufacturing availability and simultaneously be an optimum compliant mechanism design? In other words, it is required to modify the situation of Figure 11 to the state of Figure 12 that conforms to the model of single-axis flexure in Figure 7. At first, one needs carefully to measure the size of Figure 10 and re-sketch it by skilled engineer to be a much smooth configuration. Some dimensions are fixed and other dimensions surrounding the hinge-like portions need to be determined by the designer. A proposed post-optimization modeling is developed in this paper along magnifying the middle portion of micro-gripper, as shown in Figure 13 and expressed in a half configuration because of symmetry. There are two single-axis flexure hinges required to be design in a half micro-gripper.

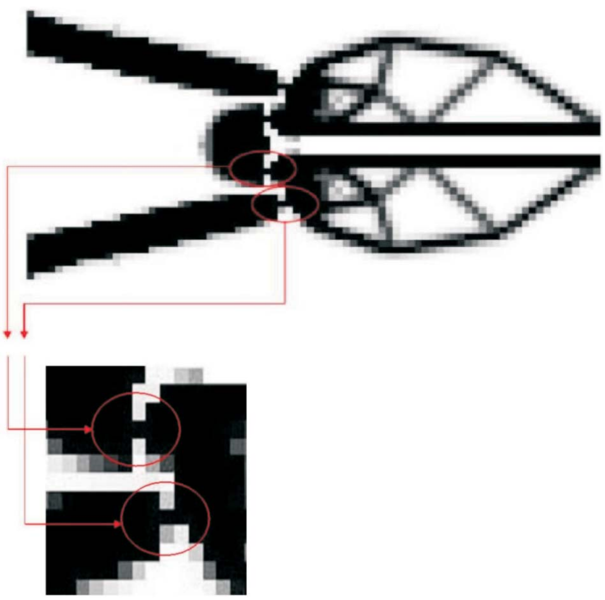

Figure 11. Hinge-like portion of micro gripper by topology synthesis.

Figure 12. Compliant flexure hinge.

Nine parameters written in l_1, θ, t_1, t_2, r_2, r_1, C_x, d_1 and d_2 are selected as design variables, represented in $X = [x_1, x_2, \ldots, x_9]^T$ and can be recognized in Figure 13. The l_1 represents the distance between two flexures centers. The angle is between l_1 and horizontal line. Parameters t_1 and t_2 are thickness corresponding two flexures. Parameters r_1 and r_2 represent radius of two flexures holes. The distance C_x is between the center of left hinge and the edge of output. Parameters d_1 and d_2 represent the distance between the periphery of hinge circle to left edge and the center, respectively.

Once a horizontal input force toward left applies to the gripper, an obviously vertical output displacement can be resulted. From the structure in Figure 13, the effects of both equivalent torsional springs stiffness should be small in order to create a maximum output motion. Therefore, the equivalent torsional spring rate $K_{\theta 1}$ and $K_{\theta 2}$, as expressed in Eq. (8–9), require to be minimized.

$$K_{\theta 1} \approx \frac{2Eht_1^{2.5}}{9\pi r_1^{0.5}} \tag{8}$$

$$K_{\theta 2} \approx \frac{2Eht_2^{2.5}}{9\pi r_2^{0.5}} \tag{9}$$

The linear stiffness of outside hinge requires a minimum stiffness, as written in Eq. (10).

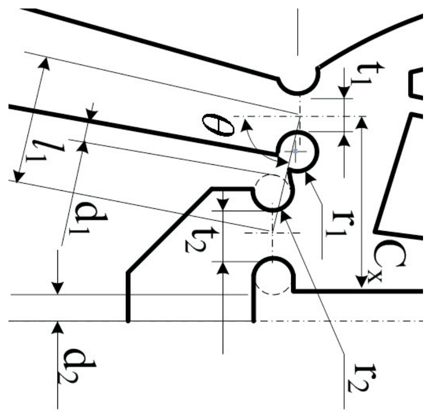

Figure 13. Design model of magnifying middle-sketch of micro gripper.

$$K_{y1} \approx \frac{2Eht_1^{2.5}}{9\pi r_1^{1.5}} \tag{10}$$

Similarly, the linear stiffness of inside hinge requires a maximum stiffness, as written in Eq. (11), in shear direction for no flexure motion generated.

$$K_{y2} \approx \frac{2Eht_2^{2.5}}{9\pi r_2^{1.5}} \tag{11}$$

The input-output relation can be derived by a small geometrical motion analysis expressed in Figure 14. The relation of output displacement ΔO_x and ΔO_y to input displacement Δi can be written as:

$$\frac{\Delta O_x}{\Delta i} = \frac{l_1 \cos\theta_1 + l_2 \cos\beta}{l_1 \sin\theta_1} \tag{12}$$

$$\frac{\Delta O_y}{\Delta i} = \frac{l_2 \sin\beta}{l_1 \sin\theta_1} \tag{13}$$

To maintain the stable grasping effect, the output vertical displacement should be large and the output horizontal displacement should be small, as compare to input horizontal displacement. This means that magnification factor (MF) of $\frac{\Delta O_x}{\Delta i}$ requires to be maximized and MF of $\frac{\Delta O_y}{\Delta i}$ requires to be minimized.

For a reasonable layout of two flexure hinges are arranged side by side, the center distance between circular holes of flexure are geometrically considered as:

$$l_1 \sin\theta - \frac{t_1}{2} - \frac{t_2}{2} - r_2 \geq 2r_1 \tag{14}$$

For preventing the relative position among r_2 and d_1 that is restricted as:

$$\sqrt{\left(l_1 \sin\theta_1 - r_2 - r_1 - \frac{t_1}{2} - \frac{t_2}{2}\right)^2 + \left(l_1 \cos\theta - r_1\right)^2} \times \sin\left\{80^\circ - \tan^{-1}\left(\frac{l_1 \cos\theta - r_1}{l_1 \sin\theta - r_2 - r_1 - \frac{t_1}{2} - \frac{t_2}{2}}\right)\right\} - r_2 - d_1 \geq 0 \tag{15}$$

For the distance of two flexure hinges has to be larger than the radius of outside circle, the constraint is written as:

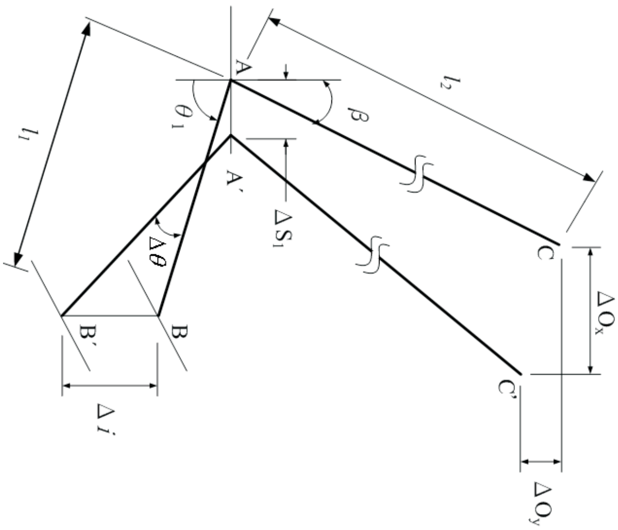

Figure 14. Geometrical motion analysis of the half gripper structure.

$$l_1 \cos\theta - r_1 \geq 0 \tag{16}$$

For controlling the outside circle of flexure hinge is within the boundary, a constraint can be formulated as:

$$C_x + 0.06 \geq l_1 \sin\theta_1 + \frac{t_2}{2} + 2r_2 + x_9 \tag{17}$$

To control the relation of two flexures, the following constraint is:

$$l_1 \sin\theta - \frac{t_1}{2} - \frac{t_2}{2} - r_1 - r_2 \leq r_1 + r_2 \tag{18}$$

Similarly, for defining the horizontal relation between two flexure hinges, the following constraint is:

$$l_1 \cos\theta_1 - (r_1 - r_2) \leq 0 \tag{19}$$

The length along flexure is restricted in the initial configuration of previous topology synthesis:

$$0.873 - \frac{1.383}{\tan 74^\circ} = C_x + 0.06 + \frac{t_1}{2} + r_1 \tag{20}$$

Some specified parameters in constrained function are measured and obtained from the topology optimization of the first design phase. Therefore, from the above description, this optimization problem is formulated as: determine nine design variables, six objective performances

(Eqs. 8−13), six inequality constraints (Eqs. 14−19) and one equality-constraint (Eq. 20). A multi-objective optimization technique is used for solving current problem.

5. Post-Optimum Result and Analysis of Mechanical Amplifier

This problem formulation is a multi-objective optimization that has been solved by Global criterion approach [16] in this paper. The optimum result is written as: $[l_1, \theta, t_1, t_2, r_2, r_1, C_x, d_1, d_2]^T = [0.2336, 72.85°, 0.0400, 0.0503, 0.0400, 0.0690, 0.3274, 0.0261, 0.0026]^T$. The final configuration of optimum micro-gripper is sketched in Figure 15. The optimum half portion surrounding the flexure hinge is clearly expressed in Figure 16.

Finite element analysis software ANSYS has been used to evaluate the performances of micro gripper design. Figure 17 shows the finite element model where the arrow is the input load direction. Figure 18 is the result after finite element analysis. The input displacement is 19.64 μm and output displacement is 139.01 μm, thus the magnification factor (MF) is 7.077. The same finite element analysis applied to the design before post-optimization to obtain the input displacement is 6.22 μm and output displacement is 35.99 μm, thus, the value of MF is 5.788. Therefore, the post-design treatment after topology optimization increases the MF with 22.3%. It is noted in original work that Tsao's thesis used pseudo-rigid-body-model (PRBM) and parametric size optimization to obtain 3.593 of MF. One compares both results and finds that the presenting design tremendously increases the MF of 97%. Furthermore, topology synthesis

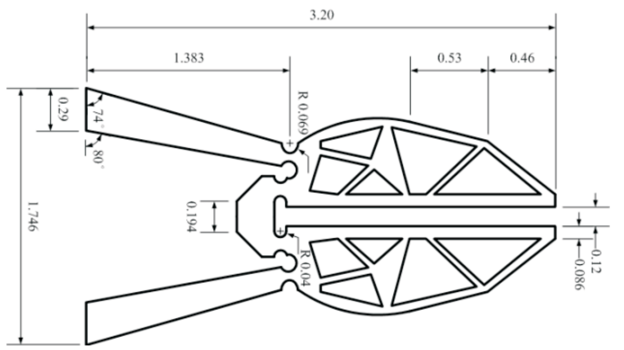

Figure 15. Post-optimum design after topological synthesis of the micro gripper.

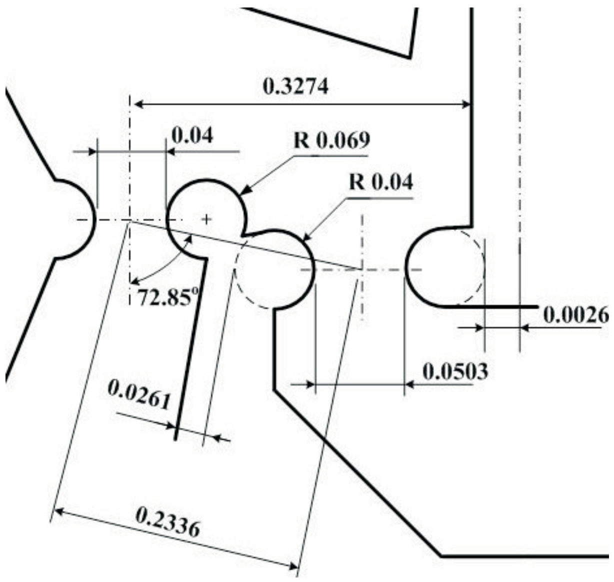

Figure 16. Optimum design surrounding flexure hinges.

Figure 17. Finite element model for micro gripper design.

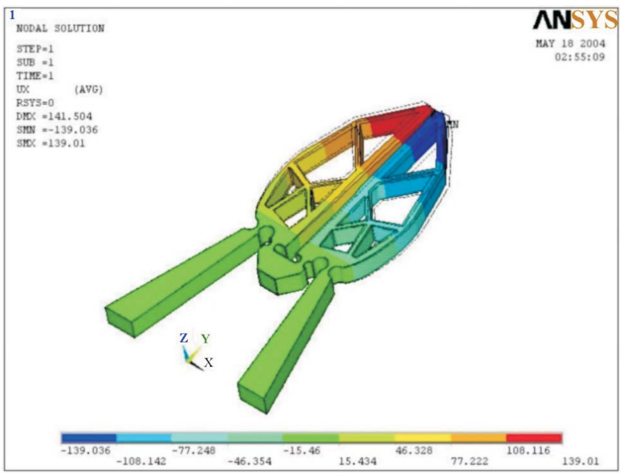

Figure 18. The result of finite element analysis for micro gripper design.

has a larger MF than PRBM with 61%. Thus, topology synthesis is an effective approach to generate an initial configuration for monolithic compliant mechanism.

6. Conclusion

The presenting paper introduces a post-optimization of handling flexure hinges design for monolithic compliant mechanism after the topology synthesis. The geometry and mathematical model of the post-design are on the basis of analytical mechanics of single-axis mechanical flexure hinge. A one-piece compliant amplifying micro-gripper has been adopted to represent the design model further illustrated the presenting approach. The final performance shows that magnification factor of output displacement to input displacement is apparently improved. The performance of topology synthesis also has been verified to be an effective approach for generating monolithic compliant structure. In this paper, we conclude that the combination of flexure hinges and structural optimization in a phase for design one-piece micro compliant mechanism is practically success. The presenting concept and post-design approach after topology optimization can be applied to general compliant mechanism synthesis.

Acknowledgement

The support received from the National Science Council, Taiwan under Grant No. NSC 92-2212-E-032-014 and NSC 93-2212-E-032-013, is gratefully acknowledged.

References

[1] Sigmund, O., "On the Design of Compliant Mechanisms Using Topology Optimization," *MECH. STRUCT. & MACH.,* Vol. 25, pp. 493–524 (1997).

[2] Kota, S., Hetrick, J., Li, Z. and Saggere, L., "Tailoring Unconventional Actuators Using Compliant Transmissions: Design Methods and Applications," *IEEE/ASME Transactions on Mechatronics,* Vol. 4 (1999).

[3] Nishiwaki, S., Frecker, M. I., Min, S. and Kikuchi, N, "Topology Optimization of Compliant mechanisms Using the Homogenization Method," *Int. J. Numer. Meth. Eng.*, Vol. 42, pp. 535–559 (1998).

[4] Pedersen, C. B.W., Buhl, T. and Sigmund, O., "Topology Synthesis of Large-Displacement Compliant Mechanisms," *Int. J. Numer. Meth. Eng.*, Vol. 50, pp. 2683–2705 (2001).

[5] Oh, Y. S., Lee, W. H., Stephanow, H. E. and Skidmore, G. D., "Design, Optimization, and Experiments of Compliant Micro gripper," *Proceedings of ASME International Mechanical Engineering Congress*, Washinton, D. C., November 15–21 (2003).

[6] Pedersen, C. B. and Seshia, A. A., "On the Optimization of Compliant Force Amplifier Mechanisms for Surface Micromachined Resonant Accelerometers," *J. Micromech. Microeng,* Vol. 14, pp. 1281–1293 (2004).

[7] Du, H., Lau, G. K., Lim, M. K. and Qui, J., "Topological Optimization of Mechanical Amplifiers for Piezoelectric Actuators Under Dynamic Motion," *Smart Mater. Struc.*, Vol. 9, pp. 788–800 (2000).

[8] Diaz, A. R. and Sigmund, O., "Checkboard Patterns in Layout Optimization," *Struct Optim,* Vol. 10, pp. 40–45 (1995).

[9] Yoon, G. H., Kim, Y. Y., BendsØe, M. P. and Sigmund, O., "Hinge-Free Topology Optimization with Embedded Translation-Invariant Differentiable Wavelet Shrinkage," *Struct Multidisc Optim*, Vol. 27, pp. 139–150 (2004).

[10] Borrvall, T., "Topology Optimization Using regularized Intermediate Density Control," *Comput Methods Appl mech Eng*, Vol. 190, pp. 4911–4928 (2001).

[11] Poulsen, T. A., "A Simple Scheme to Prevent Checkerboard Patterns and One-node Connected Hinges in Topology Optimization," *Struct Multidisc Optim*, Vol. 24, pp. 396–399 (2002).

[12] Poulsen, T. A., "A New Scheme for Imposing a Minimum Length Scale in Topology Optimization," *Int J Numer Methods Eng*., Vol. 57, pp. 741–760 (2003).

[13] Chen, W. and Lin, W., "Design of a Flexure-based Gripper Used in Optical Fiber Handling," *IEEE International Conference on Robotics, Automation and Mechatronics* (ICRAM 2004), Singapore, 1–3 December (2004).

[14] Paros, J. M. and Weisbord, L., "How to Design Flexure Hinges," *Machine Design*, November 25, pp. 151–156 (1965).

[15] Tsao, C. Y., "Design, Analysis and Testing of Micro Assembly Systems," Master thesis, Department of Mechanical Engineering, National Cheng Kung University, Taiwan, R.O.C. (2000).

[16] Shih, C. J. and Hajela, P., "Multi-criterion Optimum Design of Belleville Spring Stacks with Discrete and Integer Decision Variables," *Engineering Optimization*, Vol. 15, pp. 43–55 (1989).

Manuscript Received: Mar. 24, 2005
Accepted: Sep. 16, 2005